

Finite Element Modeling of Non-Loaded Reinforced Concrete One-Way Slab Exposed to Fire

Norlizan Wahid¹ and Tim Stratford²

¹*School of Civil Engineering, University Teknologi MARA, Cawangan Pulau Pinang, Kampus Permatang Pauh, 13500 Pulau Pinang, Malaysia.*

²*School of Engineering, The University of Edinburgh, Edinburgh, Scotland.*

*Corresponding author: ¹*norlizanwahid@uitm.edu.my*

ARTICLE HISTORY

ABSTRACT

Received
11 January 2022

Accepted
28 February 2022

Available online
31 March 2022

A study on the reinforced concrete slab behaviour at a high temperature can be done by modelling the structure using the finite element method. Different types of elements can be used to model the slab, but the effectiveness of each of the elements and the differences in the results obtained need to be studied. This study examined the differences in results obtained from the slab model built from different types of elements available in the finite element analysis. A non-loaded 250 mm thick one-way reinforced concrete slab exposed to ISO834 fire, from the study by Cooke (2001)[1], was analysed using the finite element method in Abaqus. The model builds with three different types of elements, namely plane strain, shell elements and solid elements, to distinguish their ability in predicting the slab behaviour at high temperatures. reasonablyThe mesh convergence study determined the optimum size of each element that could well predict the slab deflection within a reasonable time. A coarser mesh size of solid elements was chosen because of the computational cost limitation. The results demonstrate that different types of elements do not give a significant difference in producing temperature profiles. The slab deflection predicted by the three elements were close and comparable with the test results.

Keywords: *finite element, concrete; deflection; high temperature; Abaqus.*

1. INTRODUCTION

Finite element (FE) modelling on reinforced concrete (RC) slabs in the fire have become more common as it could provide comparable results with the experimental test. It has been widely used to analyse the high-temperature behaviour of various slabs where the FE prediction was in good agreement with the test results [2-6]. However, FE modelling of RC slabs in fire is not as straightforward as it is, depending on several factors that need to be considered. It is a complex process that deals with different material properties, nonlinearity responses and convergence problems. Furthermore, computer performance can also be a limitation since the time spent on analysis depends on it.

The slab can be modelled to obtain good results close to the actual behaviour using three-dimension solid elements as been used in previous studies [7–11]. It can reduce the assumptions made when developing the model since the shape is similar to the actual slab. The time for analysis and the size of the result's file can be significantly increased with solid elements since it contain a higher number of elements. Other researchers [4, 6, 12] prefer to use shell elements when modelling slab structures when computer performance or time become limitations. The simplest method uses the plane strain modelling concept[15] for the slab. It is useful when the time is limited and a quick result is required from the analysis. Despite the applicability of these

elements in modelling a slab structure, the difference in results obtained and their ability to predict the slab behaviour is not yet highlighted by any previous studies.

Thus, this study was carried out to investigate the variations in results derived from slab models constructed using various types of elements available in finite element analysis. The optimum arrangement of FE modelling for RC slab behaviour at high temperature was determined by looking at a different type of elements used and their size. Their ability in predicting RC slab behaviour at a high temperature close to the test results with a considerable time spent for analysis was distinguished.

1.1 The sample

A high-temperature test of 250 mm thick of non-loaded one-way RC slab done by Cook (2001) was considered and modelled using Abaqus. It was a 4.7 m long and 0.925 m wide slab, simply supported at a 4.5 m span with test arrangement as shown in Figure 1. The slab was exposed to Standard ISO 834 Fire for two hours. The effects of different parameters on the temperature profile, midspan deflection, and axial displacement of the slabs were studied [1]. The sample was chosen because it was a simple one-way slab exposed to fire without any loading. Thus, it can reduce the factors contributing to the difference between the actual test result and the prediction by FE modelling.

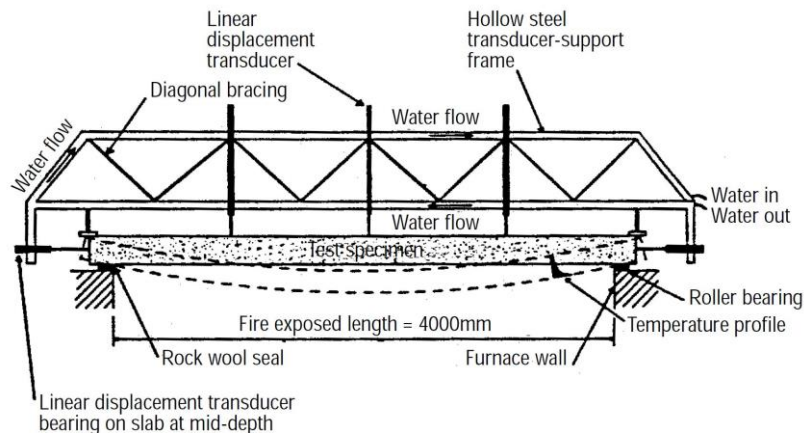


Figure 1: Experimental Arrangement of the One-Way Slab [1]

Regular weight concrete with siliceous aggregate was used in the mix, and the properties were as listed in Table 1. Six numbers of primary (longitudinal) steel bars were used, and the secondary (lateral) steel bars were laid on top of the primary steel at 90°.

Table 1: Properties of Concrete Mixes

Concrete		Steel	
Characteristic strength:	30 N/mm ²	Yield strength:	460 N/mm ²
Density:	2400 kg/m ³	Density:	1800 kg/m ³
Moisture content:	3.5%	Size:	8 mm
Thickness:	250 mm	No. of Rebars:	6
Cover:	25 mm		

2. FINITE ELEMENT MODELLING

Three different elements were used in the FE modelling: plane strain model, shell element, and solid element models. The objectives were to build an FE model that produced reliable results and to study the differences in the results produced by these three different types of elements. A Mesh convergence study was conducted by considering four different sizes of each element, as listed in Table 2. Several element layers specified the mesh sizes over the slab thickness (T) for plane strain and solid element model and division over the slab edge (E) length for shell element model.

The sequentially thermo-mechanical analysis was adopted in this study with the assumption that the stress and displacement response are dependent on the temperature values without any reverse dependency. Heat transfer analysis was first conducted for this technique, followed by the *static* analysis.

Table 2: Variation of Element Sizes and Degree of Freedoms.

Element	Plane strain		Shell element			Solid Element		
	Size (mm)	D.o.f.	Element	Size (mm)	D.o.f.	Element	Size (mm)	D.o.f.
T/8	31.3	1520	E/4	115.6	630	T/4	62.5	5010
T/10	25.0	2278	E/6	77.1	1302	T/6	41.7	11205
T/12	20.8	3200	E/8	57.5	2268	T/8	31.3	33786
T/14	17.9	4266	E/10	46.3	3366	T/10	25.0	51456

As in the test [1], an ISO 834 standard fire was applied at the bottom of the slab model for two hours. . It resulted in a maximum surface temperature that has good agreement with the test [1]. Apart from the unexposed surface, heat loss was also assumed to occur at the fire exposed surface through convection and radiation process to the surrounding.

Variations of coefficients involved in *heat transfer* analysis are unique for specific experimental setups and surrounding conditions. Thus, a series of trial analyses using different coefficient values were done to determine the best agreement of FE results with the test results. Table 3 summarises the coefficients used for *heat transfer* analysis that best represent the actual results. The thermal conductivity and specific heat for the concrete and steel were formulated in the FE modelling based on the equations given in BS EN 1992-1-2 [13].

Table 3: Summary of Heat Transfer Analysis Coefficients

ISO 834 Standard Fire		Heat Losses to Surrounding	
Convection Coefficient, h (W/m ² K)	Emissivity, ϵ	Convection Coefficient, h (W/m ² K)	Emissivity, ϵ
25	0.85	9	0.85

Temperature results from the *heat transfer* analysis are then assigned to the model in *static* analysis through the 'Predefined Fields' module. Table 4 lists the Abaqus elements used in modelling the slab sample for *heat transfer* and *static* analysis.

Table 4: Elements Used in Abaqus FE Modelling [14]

	Concrete		Steel	
	Heat Transfer	Static	Heat Transfer	Static
Plane Strain	DC2D4	CPE4R	DC1D2	T2D2
Shell Elements	DS4	S4R	NA.	NA.
Solid Elements	DC3D8	C3D8R	DC1D2	T3D2

2.1 Plane Strain model

Using the two-dimensional plane strain model is the simplest way to analyse the slab sample in FE modelling. It is generally used for modelling bodies that are very thick (z-direction) relative to their lateral (x and y directions) dimensions. The external forces are constant in the z-direction, and movement in that direction is limited. As a result, the strain components in the z-direction are treated as zero [15].

The thickness of the plane strain model was taken as the width of the slab in z-direction, while the supports and deflection were restricted to the x-y plane only. The strain is set to zero, and stresses are constant through the thickness in the z-direction. Only half of the slab was modelled, as illustrated in Figure 2, taking advantage of the symmetrical dimension and loading. For symmetric boundary conditions, displacement normal to the plane of symmetry and rotation parallel to the plane is set to be zero. In the case of the plane strain model, the displacement in the x-direction and rotation in the z-axis were set to zero.

For the plane strain element model, the concrete was modelled using a four-node bilinear, reduced integration element (CPE4R) for *static* analysis and four-node linear heat transfer quadrilateral element (DC2D4) for *heat transfer* analysis. The steel was modelled using a two-node linear two-dimensional truss element (T2D2) for *static* analysis and a two-node heat transfer link element (DC1D2) for *heat transfer* analysis.

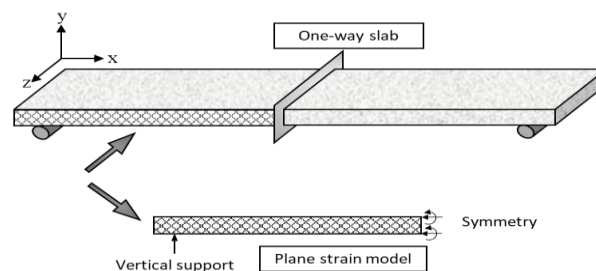


Figure 2: Development of Plane Strain Model

2.2 Shell element model

For modelling the one-way slab using a three-dimensional shell element model, only a quarter of the slab was considered in the modelling, as in Figure 3. Concrete was modelled using a four-node heat transfer quadrilateral shell (DS4) for *heat transfer* analysis and a four-node general-purpose shell element with reduced integration and hourglass control finite membrane strains (S4R) for *static* analysis. The cross-sectional behaviour of the slab was calculated using Simpson's integration rule by assigning nineteen integration points through its thickness.

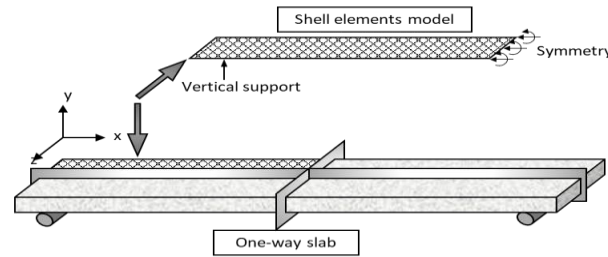


Figure 3: Development of Shell Element Model

Steel reinforcement cannot be considered during the *heat transfer* analysis of the shell element model in Abaqus [16]. However, there is a ‘Rebar Layers’ option for the static analysis in the concrete section properties unique for modelling the steel reinforcement. At this stage, Abaqus estimated the steel temperature based on the concrete temperature profile result, predefined in the *static* analysis. The steel temperature is assumed to be the same as the surrounding concrete at the same depth where the steel is located.

2.3 Solid element model

This smaller size model is vital in saving the simulation time and reducing computer memory used, especially when solid elements are to be used. Figure 4 shows the development of a quarter model of the one-way slab using a three-dimensional solid element. As boundary conditions, two symmetrical planes were assigned at the x and z axes.

Steel reinforcement was modelled using a two-node link of diffusive heat transfer elements (DC1D2) for *heat transfer* analysis and a three-dimensional two-node linear displacement truss elements (T3D2) for *static* analysis. The concrete was modelled using an eight-node linear brick of diffusive heat transfer elements (DC3D8) for *heat transfer* analysis and an eight-node linear brick with reduced integration and hourglass control (C3D8R) for the *static* analysis. A reduced integration element was used for better bending results than a fully integrated element. It is also beneficial for three-dimensional FE simulation because of its faster running time. But hourglassing instability might happen to the first-order reduced integration elements; thus, Abaqus has included control measures that should be used with a reasonably fine mesh [14]. The instability can also be controlled by distributing point load or boundary conditions to several adjacent nodes. To avoid the problem and gain reliable FE results, at least four layers of elements through the structure’s thickness are recommended for modelling the structure [17].

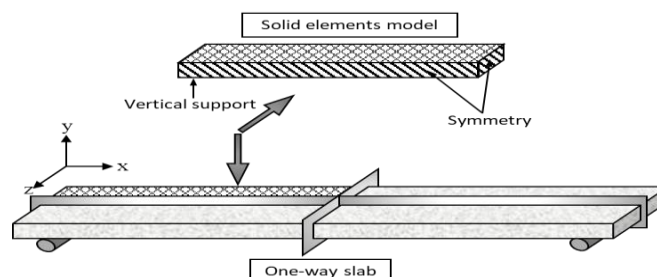


Figure 4: Development of solid element model

3. RESULTS AND DISCUSSION

3.1 Temperature Profile

Figure shows the temperature profiles at various times of fire exposure for the one-way slab predicted by FE models built from different types of elements. Generally, all predictions agreed with the test result (denoted by ‘TEST’) by Cooke (2001). The FE results demonstrate that different types of elements do not give any significant difference in producing temperature profiles. This is due to the same thermal properties and parameters used in the *heat transfer* analysis

However, it was challenging to capture the 100°C plateau pattern of the slab temperature profile because moisture movement was not explicitly modelled in the analysis. The bowing pattern was starting to appear at 30 minutes of fire exposure, approximately at a depth of 50mm to 125mm. The FE analysis had overestimated the temperature of the fire exposed surface by about 100°C at the first hour of heating. During the fire test, heat losses to the surrounding had made the exposed surface’s temperature lower than the ISO 834 standard fire temperature. The losses had been considered in the FE analysis but only shows a good agreement result with the test nearly at the end of the 120 hours exposure period.

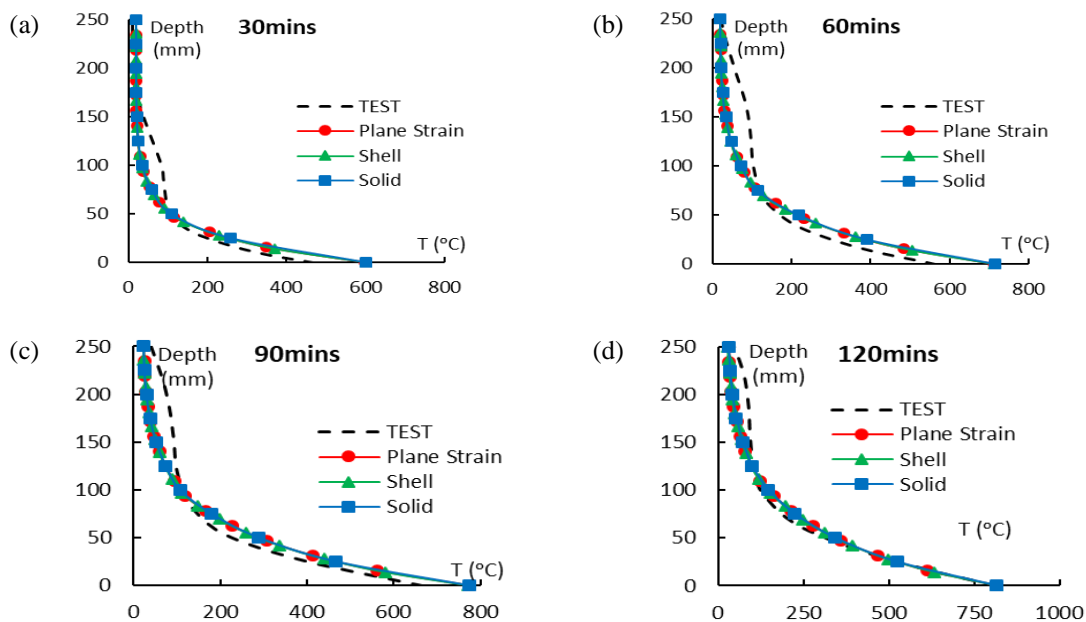


Figure 5: Temperature profiles of the one-way slab predicted by models built from different types of elements every 30 minutes.

3.2 Mesh Convergence

For the convergence study, the Central Processing Unit (CPU) time, t_{CPU} spent for executing a *static* analysis can be related to the total number of degrees of freedom (DOF), n_{dof}^{α} using the following Equation (1) [15]:

$$t_{CPU} \propto n_{dof}^{\alpha} \tag{1}$$

α is a constant with a value of 1.7 to 3.0, depending on the structure of the stiffness matrix and the solvers used in the FE method package.

Figure 6 shows the results of the mesh convergence study for one-way slab models built with different elements of plane strain, shell and solid elements. The results were shown in terms of the relationship of the total number of DOF with the final midspan deflection and CPU time spent for analysis. The CPU time spent for the three models were observed to increase proportionally with the number of freedoms complying with the relationship in Equation (1). The data for CPU time was reasonably represented by the high R-squared values for all models, ranging from 0.93 to 0.98. R-squared value is a coefficient of determination that measures how close the data are to the fitted trend-line, thus identifying the best Equation that correlates these data.

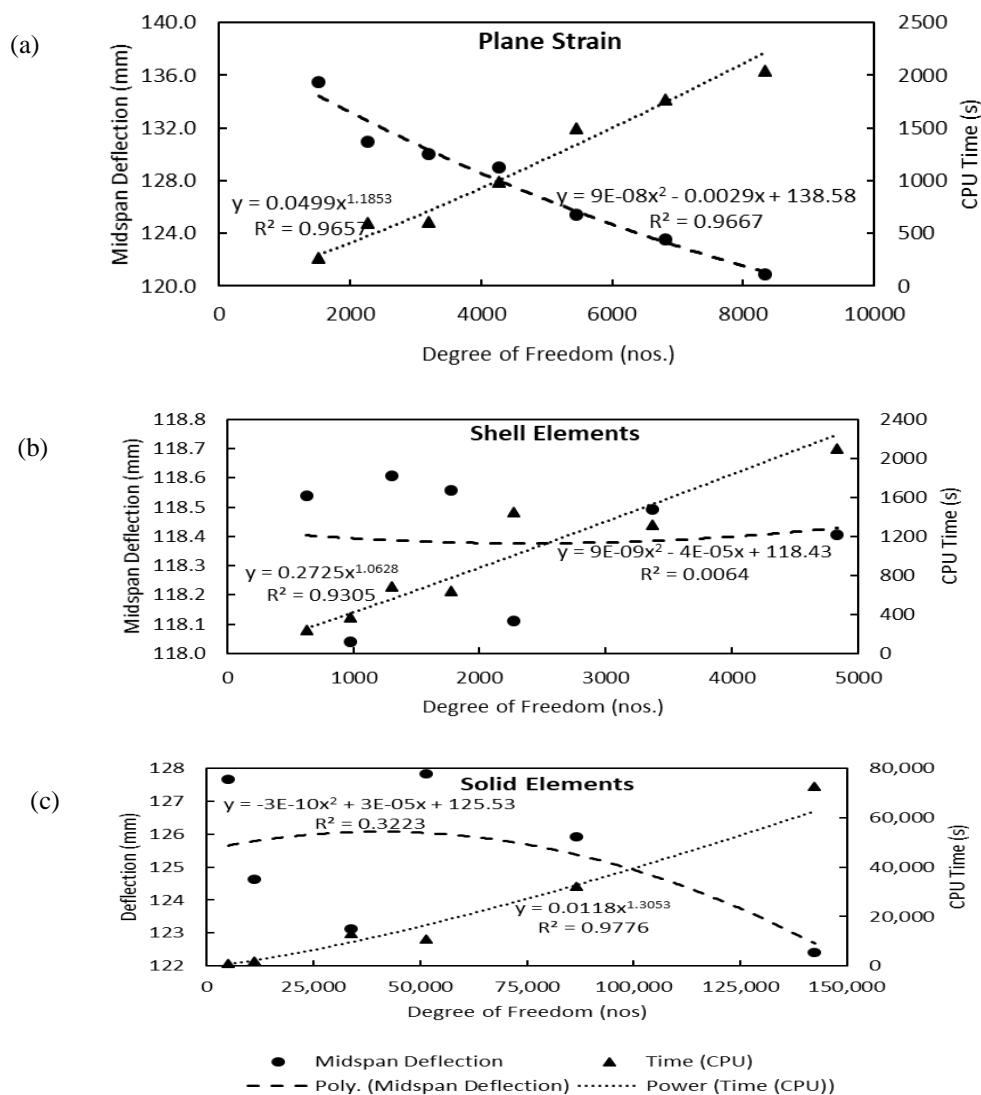


Figure 6: Relationship between the DOF numbers with midspan deflection and CPU time spend for analysis of non-loaded 250mm one-way slab build using (a) plane strain model, (b) shell elements and (c) solid elements.

The α constant was found to be the highest for solid elements, 1.305 compared to the other two of 1.063 for the shell element model and 1.185 for the plane strain model. It was contributed from the higher number of nodes for the solid element, which is eight nodes compared to 4 nodes for the shell element and plane strain model. All α constant values were smaller compared to the range given by Liu & Quek in 2003 [15]. As computer technology is growing fast nowadays, it is expected that the α constants are getting smaller over time, making it faster to complete a FE analysis. As for this study, the FE analyses were conducted in Abaqus using a 3.60GHz processor of Intel® Core™ i7-4790 with installed Random-Access Memory (RAM) of 16.0GB. The relationship between CPU Time spent with the DOF numbers can be concluded as follows:

$$t_{PS} = 0.050n^{1.185} \quad [Plane\ Strain] \quad (2)$$

$$t_{Shell} = 0.273n^{1.063} \quad [Shell] \quad (3)$$

$$t_{Solid} = 0.012n^{1.305} \quad [Solid] \quad (4)$$

The midspan data were correlated by quadratic equations based on its best R-squared values. However, the relationship between the final midspan deflection and the DOF numbers were not showing a constant pattern between different element models. Except for the plane strain model, it is difficult to conclude that the deflection results converged to one value since they scattered with low R-squared values of 0.006 for the shell elements model and 0.322 for the solid elements model. The data taken at a tiny point of the slab models at the end of fire exposure fluctuated, corresponding to the nonlinearities of the material properties at high temperatures. However, for the plane strain model in Figure 6(a), the deflection data had a better R-squared value of 0.967 and converged to a smaller deflection value with the increasing number of DOF.

Figure shows a convergence study of three different element models regarding the midspan deflection response through the 120 minutes of fire exposure time. Although the results predicted by the shell and solid elements model seen in Figure were scattered and not converging, Figure showed a constant deflection response pattern at high temperatures predicted by different mesh sizes for each element. This proves that the slab model had produced not size-dependent results when there were only slightly different between results predicted by different mesh sizes for plane strain and solid element model. While for shell elements, the predictions are almost the same. Figure portrays a better overview of a convergence study for slab models at high temperatures than the relationship shown in Figure 6. From the convergence studies, the optimum mesh sizes chosen were 25 mm, which makes ten layers of element per thickness (T/10) for plane strain, 77.1 mm, which makes six elements at its shorter edge (E/6) for the shell, and 31.25 mm, which makes eight layers of element per slab thickness (T/8) for solid element model. Table 5 shows the number of DOF and CPU time for each element size chosen, calculated using Equations (2) to (4).

Table 5: Details of the chosen mesh sizes.

Element	Size (mm)	Degree of freedom (nos.)	CPU Time (s)
Plane Strain (CPE4R)	25 (T/10)	2278	476
Shell (S4R)	77.1 (E/6)	1302	558
Solid (C3D8R)	31.25 (T/8)	51456	16889

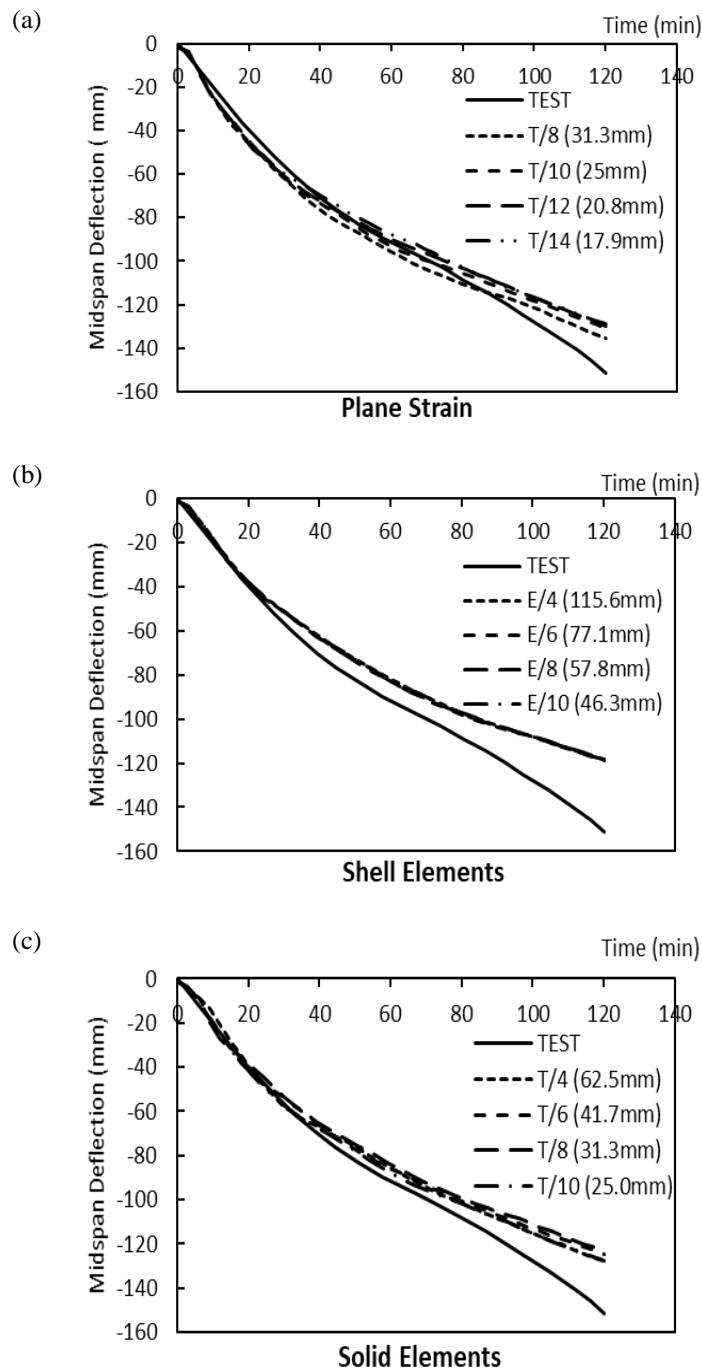


Figure 7: Midspan deflection response of a non-loaded 250mm one-way slab [1] from the model with different mesh sizes built from (a) plane strain model, (b) shell elements and (c) solid elements

A coarser mesh size of solid elements was chosen because of the computational cost limitation. CPU time taken for the analysis using the solid element model in Table 5 was already shown more than 30 times in the analysis using the other two models. Thus 31.25 mm mesh size of the solid element was used since it had produced a comparable deflection response within a reasonable CPU time. This computational cost is one of the critical factors that need to be considered when choosing a type of element and size of the mesh to be used in FE modelling.

3.3 Deflection response

Figure 85 shows the midspan deflection of the non-loaded RC one-way slab exposed to fire predicted by the three different element models. All were seen close to each other and in good agreement with the experimental test. The close prediction shows that all the types of elements could similarly represent the slab behaviour at high temperature without any significant difference. The FE predictions were starting to slightly underestimate the deflection results approximately after forty minutes of fire exposure, and the underestimations were increasingly notable towards the end. The underestimation might be caused by other factors in modelling, like the model for the material properties or the assumption of the boundary conditions, which were not covered in this study.

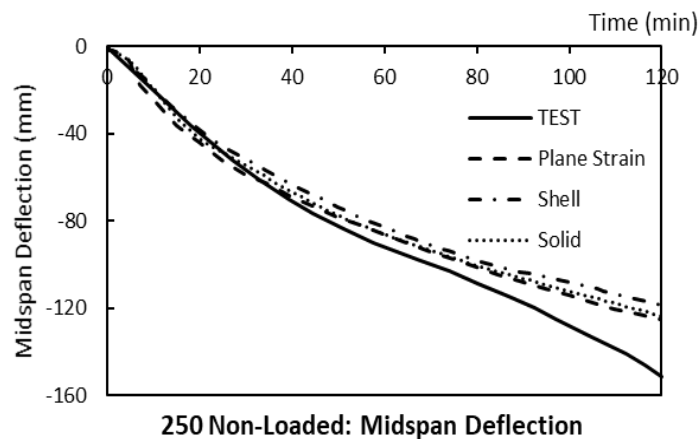


Figure 85: Midspan deflection response of a non-loaded 250mm one-way slab [1] predicted by models built using different elements.

4. CONCLUSION

The differences in FE predictions obtained from a slab model built with three different types of element models, which were plane strain, shell and solid elements, were determined in this study. The temperature profile through slab thickness had been predicted well by all the three models, and different types of an element do not give a significant difference to it. The excellent agreement between FE prediction and the experimental result was acquired by considering heat loss existence at the fire exposed surface of the slab. The heat from the heat source was not 100% transferred to the exposed surface as some had lost to the surroundings, and its magnitude is distinct for different heat transfer cases. This shows the importance of considering heat loss in modelling a heat transfer analysis from the heat source to the exposed surface.

A Mesh convergence study for deflection analysis at high temperature should also look at the overall deflection behaviour through the fire exposure time. Except for the plane strain model, the relationship between final midspan deflection with the DOF number was not precisely converged, thus making it hard to choose the suitable mesh size with the optimum CPU time spent for analysis. In general, the three FE models built using plane strain, shell and solid elements can model the one-way RC slab at high temperature. At least, for the slab deflection response, results from the models were close to each other and comparable with the experimental results, only that the solid element model takes a longer time to analyse because of the higher DOF number.

REFERENCES

- [1] G. M. E. Cooke, "Behaviour of precast concrete floor slabs exposed to standardised fires," *Fire Saf. J.*, vol. 36, no. 5, pp. 459–475, 2001.
- [2] M. Ghoreishi, A. Bagchi, and M. A. Sultan, "Punching Shear Behavior of Concrete Flat Slabs in Elevated Temperature and Fire," *Adv. Struct. Eng.*, vol. 18, no. 5, pp. 659–674, 2015.
- [3] A. Balaji, P. Nagarajan, and T. M. Madhavan Pillai, "Predicting the response of reinforced concrete slab exposed to fire and validation with IS456 (2000) and Eurocode 2 (2004) provisions," *Alexandria Eng. J.*, vol. 55, no. 3, pp. 2699–2707, 2016.
- [4] E. Baharudin, I. Rickard, L. Bisby, and T. Stratford, "Modelling Reinforced Concrete Slabs In Furnace Tests: Validation & Sensitivity To Input Parameters," in *IFireSS 2017 – 2nd International Fire Safety Symposium*, pp. 695–702, 2017.
- [5] F. Ali, A. Nadjai, and A. Abu-Tair, "Explosive spalling of normal strength concrete slabs subjected to severe fire," *Mater. Struct.*, vol. 44, no. 5, pp. 943–956, 2011.
- [6] L. Lim, A. Buchanan, P. Moss, and J.-M. Franssen, "Numerical modelling of two-way reinforced concrete slabs in fire," *Eng. Struct.*, vol. 26, no. 8, pp. 1081–1091, Jul. 2004.
- [7] D. Wang, Y. Dong, D. Zhang, W. Wang, and X. Lu, "Punching shear performance of concrete slabs under fire," *Eng. Struct.*, vol. 225, no. July, p. 111094, 2020.
- [8] B. L. Wahalathantri, D. P. Thambiratnam, T. H. T. Chan, and S. Fawzia, "A material model for flexural crack simulation in reinforced concrete elements using ABAQUS," *First Int. Conf. Eng. Des. Dev. Built Environ. Sustain. Wellbeing*, pp. 260–264, 2011.
- [9] Z. Huang, I. W. Burgess, and R. J. Plank, "Modeling Membrane Action of Concrete Slabs in Composite Buildings in Fire.I:Theroretical development," *J. Struct. Eng.*, vol. 129, no. 8, pp. 1103–1112, 2003.
- [10] N. Wahid, T. Stratford, and L. Bisby, "Calibration of concrete damage plasticity model parameters for high temperature modelling of reinforced concrete flat slabs in fire," in *Applications of Structural Fire Engineering 2019, Singapore*, no. June. 2019.
- [11] R. K. S. Al-Hamd, M. Gillie, S. A. Mohamad, and L. S. Cunningham, "Influence of loading ratio on flat slab connections at elevated temperature: A numerical study," *Front. Struct. Civ. Eng.*, vol. 14, no. 3, pp. 664–674, 2020.
- [12] E. Baharudin, L. Bisby, and T. Stratford, "Modelling the response of simply-supported two-way reinforced concrete slabs exposed to fire," *Key Eng. Mater.*, vol. 711, pp. 588–595, 2016.
- [13] British Standards Institution, *Eurocode 2: Design of concrete structures. Part 1-2: General rules — Structural fire design*, vol. 3, no. 1. U.K.: British Standards Institution, 2004.
- [14] Dassault Systèmes, *Abaqus Analysis User's Manual*. Providence, RI, USA.: Dassault Systèmes Simulia Corp., 2012.
- [15] G. R. Liu and S. S. Quek, "The Finite Element Method: A Practical Course," *Butterworth Heinemann*, p. 348, 2003.
- [16] D. Systemes, "Abaqus Unified FEA," 2013. <https://www.intrinsys.com/software/simulia/abaqus-unified-fea> (accessed Aug. 15, 2018).
- [17] E. Qiuli Sun, "Shear locking and hourglassing in MSC Nastran, ABAQUS, and ANSYS," 2006, [Online]. Available: citeulike-article-id:10361754.